

# Protein-Functionalized Gold Nanoparticles as Refractometric Nanoplasmonic Sensors for the Detection of Proteolytic Activity of *Porphyromonas gingivalis*

Anna Svärd, Jessica Neilands, Eleonor Palm, Gunnel Svensäter, Torbjörn Bengtsson, and Daniel Aili\*



Cite This: *ACS Appl. Nano Mater.* 2020, 3, 9822–9830



Read Online

ACCESS |



Metrics & More

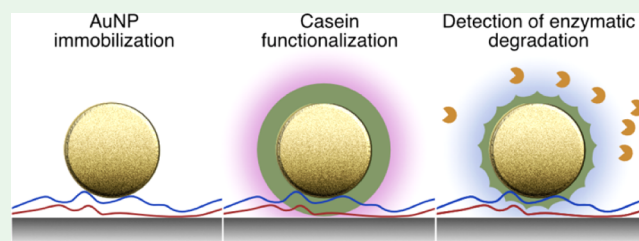


Article Recommendations



Supporting Information

**ABSTRACT:** Periodontitis is an inflammatory oral disease that affects a large part of the adult population, causing significant costs and suffering. The key pathogen, *Porphyromonas gingivalis*, secretes gingipains, which are highly destructive proteases and the most important virulence factors in the pathogenesis of the disease. Currently, periodontitis is diagnosed mainly by mechanical manual probing and radiography, often when the disease has already progressed significantly. The possibilities of detecting gingipain activity in gingival fluid could enable early-stage diagnosis and facilitate treatment. Here, we describe a sensitive nanoparticle-based nanoplasmonic biosensor for the detection of the proteolytic activity of gingipains. Gold nanoparticles (AuNPs) were self-assembled as a submonolayer in multiwell plates and further modified with casein or IgG. The proteolytic degradation of the protein coating was tracked by monitoring the shift in the localized surface plasmon resonance (LSPR) peak position. The sensor performance was investigated using model systems with trypsin and purified gingipains (subtypes Kgp and RgpB) and further validated using supernatants from cultures of *P. gingivalis*. Proteolytic degradation by proteases in buffer results in a concentration- and time-dependent blueshift of the LSPR band of about 1–2 nm when using casein as a substrate. In bacterial supernatants, the degradation of the protein coating resulted in unspecific binding of proteins present in the complex sample matrix to the nanoparticles, which instead triggered a redshift of about 2 nm of the LSPR band. A significant LSPR shift was seen only in samples with gingipain activity. The sensor showed a limit of detection < 0.1  $\mu\text{g}/\text{mL}$  (4.3 nM), which is well below gingipain concentrations detected in severe chronic periodontitis cases ( $\sim 50 \mu\text{g}/\text{mL}$ ). This work shows the possibility of developing cost-effective nanoparticle-based biosensors for rapid detection of protease activity for chair-side periodontal diagnostics.



**KEYWORDS:** gold nanoparticles, localized surface plasmon resonance, gingipains, proteolytic activity, *P. gingivalis*, periodontitis

## INTRODUCTION

Periodontitis is an inflammatory oral disease with autoimmune mechanisms, which causes irreversible destruction of tooth-supportive tissues (the periodontium). As the disease progresses, the periodontium is degenerated, resulting in tooth mobility and eventually tooth loss. Inflammation of the gum tissue, gingivitis, is the precursor condition of periodontitis. The disease affects approximately 40% of the adult population, and identifying the patients at risk of developing periodontitis among gingivitis cases is currently not possible.<sup>1</sup> Periodontitis requires life-long maintenance with multiple yearly visits to dental clinics. Despite a lot of time and effort from patients as well as caretakers being put into treatment, the disease is still a major cause of tooth extractions.<sup>2</sup> In addition, pathogens present in periodontitis can spread into the body systemically, not only via the gastrointestinal tract but also by being incorporated into the blood stream.<sup>3</sup> Inflammatory compounds and bacteria from periodontitis have been found in various tissues in the body, for example, atherosclerotic plaque,<sup>4</sup> and recently also in brain tissue, linked to Alzheimer's disease.<sup>5</sup> Periodontitis is also

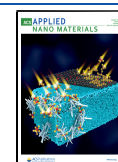
associated with numerous systemic diseases, such as cardiovascular disease,<sup>6–10</sup> rheumatoid arthritis,<sup>11</sup> and diabetes,<sup>12</sup> among others.

Some key pathogens are identified in periodontitis, among which *Porphyromonas gingivalis* is the most prominent one involved in disease progression, and it is found in over 85% of periodontal inflammation sites.<sup>13</sup> *P. gingivalis* expresses gingipains, which are a family of trypsin-like cysteine endopeptidases that are known to contribute immensely to the tissue destruction characterizing the disease.<sup>14,15</sup> Gingipains cleave peptides on the C-terminal of arginine (Rgp-subtype) or lysine (Kgp-subtype). Rgp gingipain is present in two variants, RgpA and RgpB. Whereas both RgpA and Kgp

Received: July 14, 2020

Accepted: September 16, 2020

Published: September 16, 2020



have an adhesion domain in addition to the proteolytic domain, RgpB has solely a proteolytic domain. Gingipains are primarily located in the outer membrane and in the secreted vesicles. The main function of the gingipains is to make peptides to allow bacterial growth and also to promote tissue invasion and host response modulation. Gingipains can degrade extracellular matrix proteins, activate matrix metalloproteinases (MMPs), regulate cytokines, and inactivate protease inhibitors, thereby contributing to the destruction of the periodontium and maintaining a chronic inflammatory condition.<sup>16</sup> Moreover, gingipains can act as virulence factors by, for example, degradation of antibacterial peptides and by being resistant to complement lysis due to degradation of various complement components as well as breakdown of receptors essential for phagocytosis.<sup>17,18</sup> Interestingly, gingipains have a biphasic function: when at low concentrations, they can activate the complement system to acquire nutrients for growth, and at higher levels, they degrade complement for survival and disease progression.<sup>19</sup> Previous studies have shown that gingipains account for more than 85% of the total proteolytic activity of *P. gingivalis*,<sup>20</sup> showing that these proteases are highly relevant biomarkers that not only indicate the presence of the disease but also give an idea about the disease development.<sup>21</sup> In the clinics today, there are no methods to monitor these proteases and the activity of the disease.

Periodontal diagnostics commonly used currently are bleeding on probing, probing depth, and radiographs to follow marginal bone loss.<sup>2</sup> However, these rather crude diagnostic methodologies allow the disease to progress significantly already when bone resorption has reached the stage where it is detectable. These methods are also limited with respect to sensitivity and specificity, being subjective and prone to human error.<sup>22</sup> As a complement, samples of gingival crevicular fluid (GCF) or biofilm can be sent for culturing to determine the microbiota and reveal any key pathogens.<sup>23</sup> This process is, however, time-consuming and costly, requires trained personnel, and is therefore very rarely used. Other methods aimed at detecting the presence or concentration of bacteria or gingipains for diagnostics of periodontitis have been suggested based on immunofluorescence,<sup>24</sup> polymerase chain reaction,<sup>25,26</sup> fluorescence resonance energy transfer,<sup>27</sup> and magnetic nanobeads.<sup>28</sup> However, because of the high cost and the tedious and time-consuming multistep procedures involved, none of these methods have been successfully translated to the clinic. To our knowledge, a lateral-flow immunoassay detecting MMP-8 is so far the only commercially available product that was reported.<sup>29</sup> There is consequently a need for further improved diagnostic tools that can detect the activity of the disease before substantial bone resorption occurs and that can provide information about proteolytic activity rather than just the presence or concentration of virulence factors.<sup>30</sup> This would enable an earlier onset of preventive treatment, lead to more personalized and cost-effective therapies, which would benefit both patients and caregivers, and align with the concepts of P4 medicine (predictive, preventative, personalized, and participatory). In addition to improving the health of the oral cavity, better diagnostic methods for periodontitis would possibly also mitigate systemic diseases due to the strong link between the disease and general health.<sup>3,31,32</sup>

Gold nanoparticles (AuNPs) have unique optical properties, low toxicity, stability to oxidation, and flexibility with respect to

surface chemistry and have been widely used in various biosensor applications.<sup>33,34</sup> AuNP-based detection of enzyme activity, and protease activity in particular, has primarily relied on the colorimetric response caused by changes in nanoparticle stability.<sup>35,36</sup> Aggregation of suspended AuNPs typically gives rise to pronounced redshift of the localized surface plasmon resonance (LSPR) because of the decrease in separation between individual AuNPs, resulting in plasmonic coupling. By functionalizing AuNPs with peptide-based protease substrates, protease cleavage of the peptides can trigger aggregation, prevent aggregation of destabilized nanoparticles, or disrupt already formed aggregates, resulting in a color change.<sup>35,37</sup> However, the requirement to couple specific substrate recognition with modulation of nanoparticle stability makes the assay design complicated and often involves trade-offs between analyte recognition and surface passivation. Unspecific adsorption of proteins present in complex sample matrices can thus be problematic and hinder access to the substrate and reduce the magnitude of the aggregation or even result in unspecific aggregation, making clinical translation of these colorimetric assays very difficult. Plasmonic nanostructures have also been employed for protease activity monitoring in complex sample matrices using surface enhanced Raman scattering (SERS).<sup>38</sup> Albeit sensitive, quantitative analyte detection using SERS can be challenging and requires careful calibration using internal or external standards to account for, for example, variations in substrate properties and analyte–surface interactions.<sup>39</sup> Here, we instead exploit the sensitivity of plasmonic nanoparticles to subtle changes in the refractive index (RI) in the immediate vicinity of the AuNP surface<sup>40,41</sup> for monitoring protease activity. Although the RI sensitivity ( $\eta$ ) of most types of AuNPs is quite modest ( $44 < \eta < 703$  nm/RIU), it is still possible to monitor biomolecular interactions with high precision.<sup>42</sup> LSPR-based RI biosensors are generic, do not require an internal standard, and can be based on AuNPs immobilized on a solid substrate, circumventing many of the main issues with SERS and colorimetric nanoplasmonic sensors.<sup>43</sup> However, LSPR sensors have limited sensing depth ( $\lesssim 20$  nm), and there are consequently restrictions in size of the ligands and ligand immobilization strategies that can be used. On the other hand, less problems with bulk RI changes are seen as compared to more<sup>36</sup> conventional surface plasmon resonance biosensors. The simple optical setup required for LSPR-based sensing further facilitates development of very cost-effective devices.<sup>44</sup>

Here, we have investigated the potential of LSPR-based refractometric sensing for gingipain activity monitoring using a multiwell format and a conventional plate reader as a transducer. Spherical 50 nm AuNPs were immobilized in well plates and modified with casein that served both as a generic protease substrate and as a passivating layer for preventing unspecific protein adsorption. The strategy was evaluated using trypsin, purified gingipains, and vesicle-bound gingipains from cultured bacteria. We show that it is possible to detect low concentrations of proteases by monitoring the changes in RI caused by protease-mediated remodeling of the adsorbed casein layer. Free proteases give rise to a blueshift in the LSPR peak because of digestion of the adsorbed casein. In contrast, proteolytic activity in more complex samples from bacteria cultures instead resulted in a pronounced redshift of the LSPR band, likely because of the disruption of the passivating layer resulting in unspecific adsorption. This effect was seen only in proteolytically active samples. Because of its

simplicity, this versatile strategy can facilitate further development of rapid noninvasive point-of-care methods for early detection of periodontitis and prediction of disease progression. Direct feedback to the patients can also increase awareness and thereby also increase compliance to treatment plans. In addition, the versatility of the method, combined with the flexibility of gold surface chemistry, can facilitate further development of sensors for a wide range of other proteases.

## EXPERIMENTAL SECTION

**Chemicals.** All chemicals were obtained from Sigma-Aldrich Merck KGaA (Darmstadt, Germany) without further purification, unless otherwise noted. Arginine specific gingipains (RgpB-subtype, GingisRex) and lysine-specific gingipain (Kgp-subtype, GingisKHAN) were purified from *P. gingivalis* by Genovis, Lund, Sweden.

**LSPR Sensor Design.** Spherical citrate-covered gold nanoparticles (AuNPs) with a diameter of 50 nm (BBI Solutions, USA) were immobilized in plasma-treated 96-well plates (Nunc, transparent, flat, round) according to a technique reported by Nooney et al.<sup>45</sup> The well plates were treated using oxygen plasma (0.8 mbar, 240 s, 200 W, 40 kHz generator, gas used) in a Diener Pico Plasma chamber (Diener electronics, Ebhausen, Germany), followed by adsorption of a polyelectrolyte multilayer according to a protocol reported by Decher.<sup>46</sup> Polyelectrolyte solutions of polyethylenimine (PEI,  $M_w$  750,000), polystyrene sulfonate (PSS,  $M_w$  75,000), and polyallylamine hydrochloride (PAH,  $M_w$  56,000) were prepared with a concentration of 2 mg/mL in 0.5 M NaCl in Milli-Q (MQ) water ( $18.2 \text{ M}\Omega \text{ cm}^{-1}$ ), and 100  $\mu\text{L}$  of polyelectrolyte solution was added to each well for 10 min in the order PEI/PSS/PAH/PSS/PAH with a thorough rinsing of MQ water between each deposition. Finally, 100  $\mu\text{L}$  of a gold nanoparticle suspension with a particle diameter of 50 nm (BBI solutions, USA) was added to each well and incubated for 4 h at room temperature (RT), followed by rinsing with MQ water. Three different protein coatings were evaluated: casein, immunoglobulin G (IgG) from human serum, and human serum albumin (HSA). Casein, 1 mg/mL (42  $\mu\text{M}$ ), was dissolved in MQ water because of limited solubility in most buffers and was physisorbed on the AuNPs for 30 min at RT, followed by rinsing with MQ water (>10 mL per well). IgG 1 mg/mL (6.7  $\mu\text{M}$ ) was provided in 10 mM  $\text{PO}_4^{3-}$ , 137 mM NaCl, and 2.7 mM KCl, pH 7.4 (PBS), and was physisorbed on AuNPs for 30 min at RT, followed by rinsing with MQ water (>10 mL per well). HSA, 1 mg/mL (14  $\mu\text{M}$ ), was treated in the same manner as casein and was dissolved in MQ water and physisorbed on the AuNPs for 30 min at RT, followed by rinsing with MQ water (>10 mL per well). Trypsin from bovine serum was dissolved in PBS buffer to mimic physiological ionic strength and pH and was used as a model system for investigating the degradation of the protein film (60 min incubation at 37 °C followed by rinsing with MQ water, >10 mL per well). Gingipains of Kgp (lysine-specific) dissolved in Tris with cysteine (2 mM) and Rgp (arginine-specific) dissolved in Tris with urea (4 M) and cysteine (10 mM) subtypes (Genovis, Lund, Sweden) were also evaluated (60 min incubation at 37 °C, followed by rinsing with MQ water, >10 mL per well). Data were obtained by monitoring the plasmon peak position after incubation of various proteins and proteases. UV-vis absorbance scans 400–800 nm was measured using an Infinite M1000PRO plate reader. Polyelectrolyte layers without AuNPs were measured as a background in the UV-vis measurements and subtracted prior to analysis. Data were fitted to a 9th degree polynomial using Matlab (MATLAB and Statistics Toolbox Release 2017a, The MathWorks, Inc., Natick, Massachusetts, United States) to identify the LSPR peak position. For scanning electron microscopy (SEM) measurement, spherical AuNPs (50 nm) were immobilized onto conducting glass surfaces according to the same protocol as described above, and the image was required with a LEO 1550 Gemini (Zeiss) at 5 kV acceleration voltage after sputter-coating with Pt.

**Bacterial Culture.** *P. gingivalis* wild-type (wt) W50 and W50-derived mutants, RgpA RgpB double mutant E8, and Kgp mutant K1A were kindly provided by professor M. A. Curtis, Molecular

Pathogenesis Group, Queen Mary, University of London. The strains, including *P. gingivalis* wild-type ATCC 33277 (American Type Culture Collection, Manassas, VA, USA), were grown in fastidious anaerobe broth, 29.7 g/L, pH 7.2, (Lab M Limited, Bury, UK), for 72 h under anaerobic conditions (80%  $\text{N}_2$ , 10%  $\text{CO}_2$ , and 10%  $\text{H}_2$ ) at 37 °C in an anaerobic chamber (Concept 400 Anaerobic Workstation; Ruskinn Technology Ltd., Leeds, United Kingdom). *Streptococcus mutans* was kindly provided by professor Gunnell Svensäter, Malmö University. *S. mutans* was grown in a Luria–Bertani broth (Difco Laboratories, Detroit, MI, USA) in 37 °C with 5%  $\text{CO}_2$  for 48 h. The bacterial suspensions containing  $1 \times 10^9$  cfu/mL were centrifuged for 10 min at 10,000g to prevent further increase in gingipain concentrations, and the bacteria-free supernatants were stored in a freezer prior to further analysis.

### Protease Activity Monitoring Using Fluorogenic Substrates.

A bacterial sample (100  $\mu\text{L}$ ) was added to BikKam-16 (Arg-gingipain specific substrate, final concentration 16 nM) (PepScan Presto B.V., Lelystad, The Netherlands) and fluorescein isothiocyanate (FITC)-casein substrate (0.1 mg/mL, final concentration) (QuantiCleave Fluorescent Protease Assay kit, Pierce). Proteolytic activity was monitored by measuring the fluorescence in a plate reader (Clariostar Optima) with 1 min intervals during 30 min and excitation and emission wavelengths of 488 and 538 nm, respectively. Rgp activity using BikKam-16 was expressed as relative fluorescent units/min and general proteolytic activity by using FITC-casein as final RFU after 30 min. The standard curve for Rgp was obtained as described above with five different concentrations of GingisRex used.

**Zymography.** Cell-free supernatants prepared as described above were run at 125 V, 4 °C on pre-cast Novex 10% Zymogram plus gels containing gelatin. The running buffer [25 mM Tris, 192 mM glycine, buffer pH 8.3 containing 0.5% sodium dodecyl sulfate (SDS)] was kept at 4 °C. Gels were renatured by replacement of SDS with a non-ionic detergent (25% Triton X-100) using Novex Zymogram Renaturing buffer (4 °C for 30 min), so that proteins were shifted from noncatalytic to catalytic conditions. Gels were then equilibrated with Novex Zymogram Developing buffer containing 2 mM L-cysteine for 30 min at 4 °C. Fresh developing buffer containing 2 mM L-cysteine was then added, and the gel was incubated at 37 °C for 2 h. Finally, gels were stained with colloidal Coomassie brilliant blue G overnight, and excess stain was removed in 25% ethanol in 1 h at RT. All gels and reagents were obtained from Invitrogen (Thermo Fisher Scientific, USA).

**Null-Ellipsometry.** Gold substrates were prepared by evaporating a 25 Å Ti adhesion layer followed by 2000 Å of Au on clean (111) silicon wafers in a Baltzers UMS 500 P system. The base pressure was below  $10^{-9}$  Torr, and the evaporation pressure was on the low  $10^{-7}$  Torr scale. The gold surfaces were cleaned in a mixture of 5/7  $\text{H}_2\text{O}$ , 1/7  $\text{H}_2\text{O}_2$  (30%), and 1/7  $\text{NH}_3$  (25%) at  $\sim 85$  °C for 10 min and thoroughly rinsed with MQ water prior to casein immobilization. The surfaces were incubated in 1 mg/mL casein dissolved in MQ water for 30 min at RT and rinsed thoroughly with MQ water prior to analysis. The effect of trypsin was investigated by incubating the casein-coated gold surfaces for 21 h in trypsin (0.1 mg/mL) in MQ water, followed by rinsing in MQ water. The protein film thickness was measured using null-ellipsometry on an automatic Rudolph Research AutoEL III ellipsometer with a He–Ne laser operating at 632.8 nm at an angle of incidence of 70°. An optical model based on isotropic optical constants for the protein layer  $N_{\text{prot}} = n + ik = 1.50$ , with  $n = \text{RI}$  and  $k = \text{extinction coefficient}$ , was used for the evaluation of the film thickness. Data from at least five spots on each surface were averaged.

**Data Handling.** Data analysis was performed in Microsoft Excel 2019 and Matlab (MATLAB and Statistics Toolbox Release 2017a, The MathWorks, Inc., Natick, Massachusetts, United States). Graphs were visualized in Graph Pad Prism 8 (GraphPad Software, La Jolla California USA). Data for blanks of enzyme digestion samples were subtracted prior to analysis (Figure S1, Supporting Information).

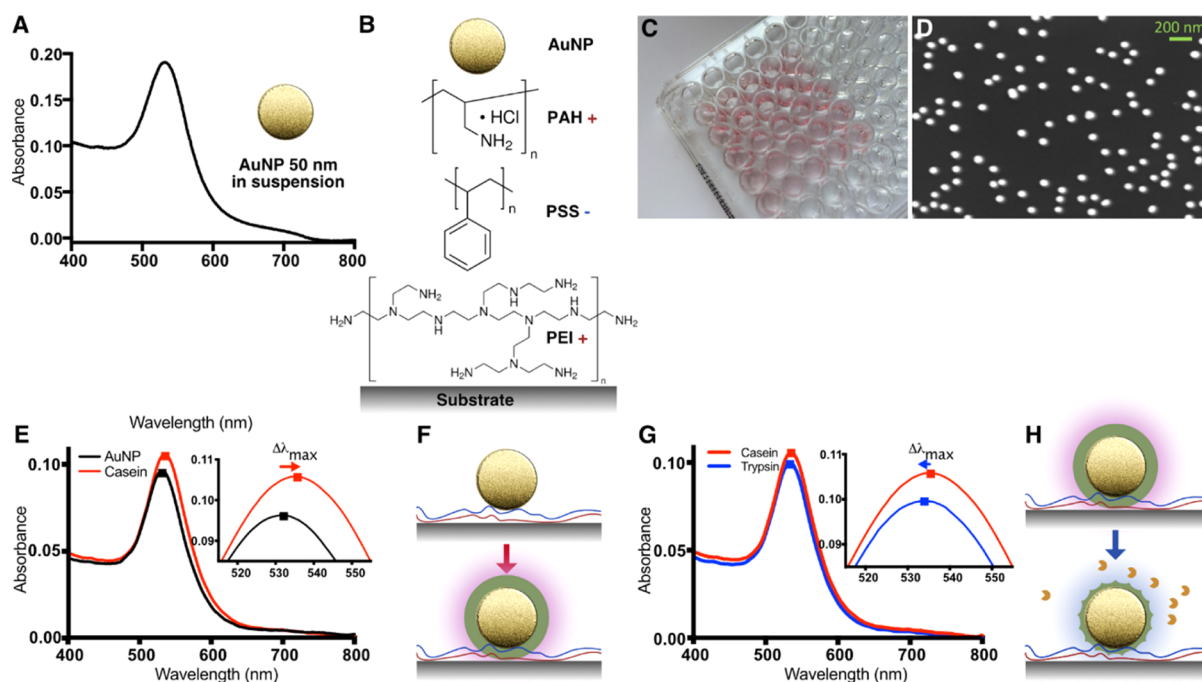


**Figure 1.** (A) UV-vis spectra of suspended AuNPs prior to immobilization. (B) Spherical AuNPs (50 nm) were immobilized in 96-well plates using a polymer adhesive layer comprising PEI, PSS, and PAH. (C) Photograph and (D) SEM of immobilized AuNPs. (E) UV-vis spectra before and after casein functionalization (inset shows a zoomed-in image of the peak position). (F) Casein functionalization of AuNPs results in an increase in the effective RI in the vicinity of the AuNP surface. (G) UV-vis spectra before and after enzymatic degradation (inset shows a zoomed-in image of the peak position). (H) Degradation of casein immobilized on the AuNPs by proteases results in a decrease in the effective RI in the vicinity of the AuNP surface.

## RESULTS AND DISCUSSION

### Sensing Surface Assembly and Characterization.

Spherical AuNPs ( $\varnothing = 50$  nm) were immobilized in 96-well plates using a polyelectrolyte adhesion layer (Figure 1A,B). Although larger AuNPs can show higher RI sensitivity, they tend to have larger size distribution, resulting in a broader LSPR band, that is, larger full width half maximum and thus a lower figure of merit.<sup>47</sup> The AuNPs were homogeneously distributed on the substrate after immobilization, which could be seen from the pink color of the plastic, scanning electron micrographs, and UV-vis spectra (Figure 1C–E). The immobilization of the AuNPs resulted in a small redshift of the LSPR peak from  $532.2 \pm 0.1$  ( $n = 5$ ) nm for the dispersed nanoparticles to  $535.3 \pm 0.1$  nm ( $n = 5$ ) after 4 h incubation at RT because of the substrate effect.<sup>48</sup> Casein (1 mg/mL) was dissolved in MilliQ-water (MQ) and was added to the wells and incubated for 30 min to assemble a casein layer on the AuNPs. The casein coating of the immobilized AuNPs (AuNP-casein) resulted in an additional redshift of the LSPR peak maximum of  $\Delta\lambda_{\max} = 3.8 \pm 0.1$  nm (Figure 1E). The adsorbed casein was used both as a generic protease substrate and to passivate the surface to prevent unspecific protein adsorption, as schematically outlined in Figure 1F. Degradation of the immobilized casein by proteolytic enzymes was expected to result in a decrease in RI in the vicinity of the AuNP and consequently a blueshift of the LSPR band.

**Detection of Trypsin.** Gingipains are often referred to as trypsin-like cysteine proteases and have a substrate preference similar to trypsin, that is, polypeptides with positively charged lysine and arginine side chains.<sup>21</sup> Trypsin was thus considered as a relevant model system for gingipains when investigating the sensor response to proteolytic degradation of the

immobilized casein. Exposing the casein-coated AuNPs to trypsin resulted in a distinct blueshift of the LSPR peak position, clearly indicating removal of material from the AuNP surface (Figure 1G,H). The trypsin response was concentration-dependent with a limit of detection (LOD) of  $<0.1$   $\mu\text{g/mL}$  (4.3 nM) (Figure 2A), where LOD is defined as the

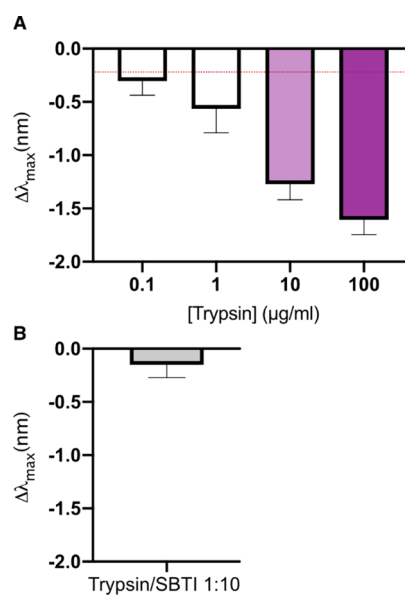


**Figure 2.** Proteolytic activity of trypsin. Mean (SD),  $n = 5$ . (A) LSPR blueshift caused by trypsin, where  $0.1$   $\mu\text{g/mL} = 4.3$  nM,  $1$   $\mu\text{g/mL} = 43$  nM,  $10$   $\mu\text{g/mL} = 430$  nM, and  $100$   $\mu\text{g/mL} = 4.3$   $\mu\text{M}$ . The red dotted line indicates LOD. (B) LSPR shift was reduced after trypsin (1 mg/mL) inactivation by SBTI (1 mg/mL) 1:10.

concentration of analyte generating a response  $>3 \times \text{SD}$  of the blank. The sensitivity is thus similar to fluorescence-based assays using FITC-labeled casein.<sup>49</sup> The magnitude of the LSPR shift was significantly reduced when the sensor surface was exposed to trypsin (1 mg/mL) in the presence of a trypsin inhibitor (soy-bean trypsin-inhibitor, SBTI) (Figure 2B). The trypsin-triggered blueshift of the LSPR peak is consequently a result of a proteolytic degradation of the physisorbed casein. The reaction was rapid, and a substantial blueshift was obtained in  $<5$  min (Figure S2, Supporting Information), but to facilitate handling and comparison between samples, a 60 min incubation was used for all samples analyzed using LSPR. The magnitude of the blueshift was not large enough to be seen by the naked eye<sup>50</sup> but was readily and reproducibly recorded using a simple bench-top plate reader. The ability of trypsin to degrade casein adsorbed on gold was further confirmed using null-ellipsometry. Incubating the casein-modified gold substrates with trypsin (100  $\mu\text{g/mL}$ , 4.3  $\mu\text{M}$ ) resulted in a decrease in film thickness from  $23.0 \pm 0.6$  to  $17.6 \pm 1.5 \text{ \AA}$  ( $n = 5$ ).

**Proteolytic Activity of Gingipains.** Exposing the casein-modified AuNPs to Kgp gave rise to a similar blueshift as trypsin ( $\Delta\lambda_{\text{max}} \approx 1\text{--}2 \text{ nm}$ ) (Figure 3A), with an LOD  $< 0.1 \mu\text{g/mL}$  (4.3 nM). Interestingly, when instead using physisorbed IgG as the substrate, a smaller blueshift of approximately  $\Delta\lambda_{\text{max}} \approx -0.5$  to  $-1 \text{ nm}$  was seen for lower concentrations ( $\leq 14 \mu\text{g/mL}$ , 130 nM) of Kgp, whereas for higher concentrations of Kgp, a more pronounced blueshift was obtained ( $\Delta\lambda_{\text{max}} \approx -3$  to  $-4 \text{ nm}$ ) (Figure 3B). The four subclasses of IgG from human serum and their proportional amounts are IgG1 (65%), IgG2 (25%), IgG3 (6%), and IgG4 (4%).<sup>51</sup> Kgp is known to readily digest IgG1;<sup>52,53</sup> however, the number of cleavage sites is restricted and primarily located in the hinge region. At lower concentrations of Kgp, the degradation of IgG is hence likely not complete within the assay time (60 min) and Kgp are also probably still associated to the substrates. The response for Rgp (subtype B) on casein-coated AuNPs was not as pronounced as for Kgp (Figure 3C). The turnover number ( $k_{\text{cat}}$ ) is similar for both enzymes, with reported values of 9.4 and  $5\text{--}50 \text{ s}^{-1}$  for Kgp<sup>54</sup> and Rgp,<sup>55</sup> respectively, but there are fewer number of potential cleavage sites in casein for Rgp than for Kgp. Beta-casein has 11 lysine residues but only 4 arginines, making cleavage by Rgp less likely and less efficient as compared to Kgp, which correlates with the LSPR data. In addition, the Rgp gingipain used in this study was subtype B, which lacks the adhesion domain which typically is involved in the association of enzyme to both other proteins and surfaces.<sup>16</sup>

**Proteolytic Activity in Supernatants from Bacteria Cultures.** Gingipains are present in both the outer membrane of the bacteria and in vesicles and, to a lower extent, in soluble forms.<sup>16,20</sup> Since *P. gingivalis* primarily reside in biofilms and the adjacent epithelium,<sup>56</sup> the membrane-bound gingipains are out of reach for a sensor. In contrast, vesicles will, to a certain extent, be present in both GCF and in saliva.<sup>57</sup> Vesicle-bound gingipains are hence the main analyte that can be targeted. To determine the proteolytic activity from *P. gingivalis* associated to vesicles, supernatants from cultures of two different strains, W50 (wild-type) and ATCC 33277, were investigated. In addition, two gingipain knock-out strains were investigated, where E8 is W50-deficient in Rgp and K1A is W50-deficient in Kgp. The caries bacteria *S. mutans* was used as a negative control. Zymography and fluorogenic substrates were used to

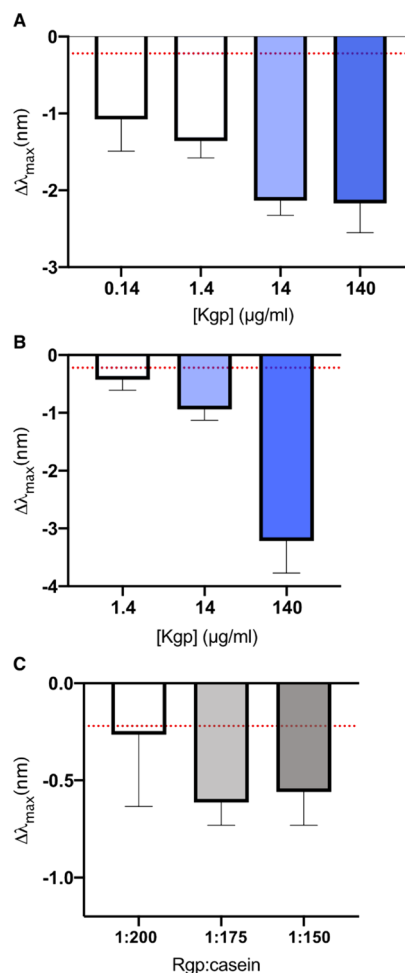


**Figure 3.** Gingipain-induced LSPR shift of protein-coated AuNPs (50 nm). Mean (SD),  $n = 5$ . (A) Kgp on casein-coated AuNPs, where  $0.14 \mu\text{g/mL} = 1.3 \text{ nM}$ ,  $1.4 \mu\text{g/mL} = 13 \text{ nM}$ ,  $14 \mu\text{g/mL} = 130 \text{ nM}$ , and  $140 \mu\text{g/mL} = 1.3 \mu\text{M}$ . (B) Kgp on IgG-coated AuNPs. (C) Rgp on casein-coated AuNPs where the ratio corresponds to an RgpB concentration of  $5 \mu\text{g/mL} = 100 \text{ nM}$  (1:200),  $5.7 \mu\text{g/mL} = 114 \text{ nM}$  (1:175), and  $6.7 \mu\text{g/mL} = 134 \text{ nM}$  (1:150). The red dotted line indicates LOD.

verify the proteolytic activity in the bacterial supernatants. The results from the zymography displayed proteolytic activity for all the different strains of *P. gingivalis*. K1A, deficient in Kgp, lacked a band present in E8 as well as W50 and ATCC with the molecular weight corresponding to that of Kgp (60 kDa). K1A also had two major bands, one  $>76 \text{ kDa}$  and the other  $<52 \text{ kDa}$ , that were lacking in E8, which would suggest that these represent RgpA and RgpB. These two bands were also present in the wild-type and strain ATCC 33277 of *P. gingivalis* (Figure 4). *S. mutans* showed no proteolytic activity as seen by absence of clear bands on the gel. The results from zymography was confirmed using the specific fluorogenic Rgp substrate BikKam-16 and FITC-casein for assessing for general proteolytic activity (Table 1). The highest Rgp activity was seen for W50, which also displayed high general proteolytic activity. The Kgp mutant (K1A) showed a similar general activity, although the Rgp activity was somewhat lower. The lowest general activity was seen for Rgp mutant E8. E8 also displayed limited activity for BiKam-16, which was expected because this is a substrate specific for Rgp. Type strain ATCC 33277 showed in general lower activity than

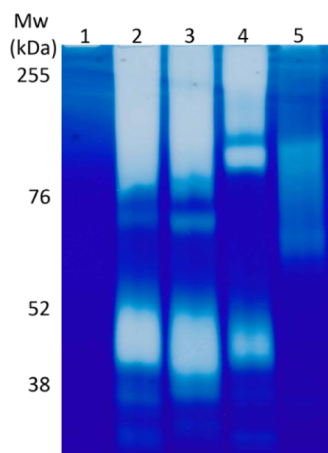


**Figure 4.** Zymogram with lanes representing (1) *S. mutans*, (2) *P. gingivalis* W50, (3) *P. gingivalis* ATCC 33277, (4) *P. gingivalis* K1A, and (5) *P. gingivalis* E8. All bacterial suspensions contained  $1 \times 10^9$  cfu/mL.

**Table 1. Proteolytic Activity of Bacterial Supernatants from *P. gingivalis* on Fluorescent Substrates BikKam-16 and FITC-Casein<sup>a</sup>**

bacteria	BikKam-16 (RFU/min)	FITC-casein (final RFU)
<i>S. mutans</i>	-1.3	2244
W50	84	12,973
ATCC	36	9493
K1A	15	13,818
E8	1.2	7753

<sup>a</sup>RFU = relative fluorescent units.

W50, with lower Rgp activity in particular. These findings support previous studies, showing that W50 is overall a more potent strain than ATCC.<sup>58</sup> ATCC 33277, on the other hand, displayed higher Rgp activity than the two mutants. As expected, *S. mutans* showed very low proteolytic activity and no activity with BikKam-16. A standard curve for Rgp was generated where Rgp was incubated with FITC-casein during 30 min (Figure S3, Supporting Information), and the equation for the linear part of the graph was used to calculate the concentration of Rgp in the samples. The final RFU value of 13,818 (K1A) corresponded to an Rgp concentration of  $1 \mu\text{g/mL}$ . This value is in the range of what one could expect to find in GCF from individuals suffering from periodontitis and within the dynamic range of the LSPR sensor. Guentsch et al. measured the Rgp amount in GCF from patients with severe chronic periodontitis.<sup>59</sup> In the 70 sites tested positive for Rgp, the median value was 1.45 ng Rgp/site with a maximum of 32 ng. 1.45 ng Rgp/site corresponds to an Rgp concentration of  $48 \mu\text{g/mL}$ , assuming that the GCF volume in a site is  $0.65 \mu\text{L}$  (as stated by Lönn et al.<sup>60</sup>). Overall, the results confirm proteolytic activity in all strains of *P. gingivalis* but not in the negative control *S. mutans* as well as Rgp activity in W50, ATCC 33277, and K1A. The results also show that the proteolytic activity of the supernatants used in this study could resemble that found in GCF samples from patients with chronic periodontitis.

**LSPR Response to Vesicle-Bound Gingipains.** In contrast to the blueshift of the LSPR response for free purified gingipains, the vesicle-bound gingipains gave rise to a pronounced redshift of the LSPR band, indicating an

accumulation of material on the nanoparticles rather than removal as expected (Figure 5A). Similar responses were seen

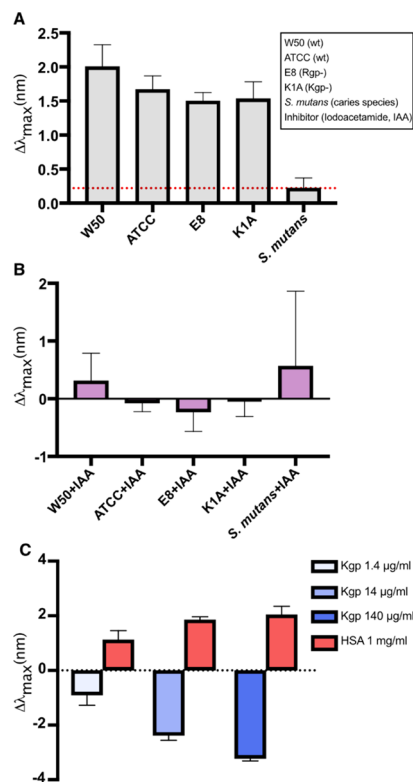


**Figure 5.** LSPR shift of casein-coated AuNPs after 60 min incubation with supernatants from bacterial cultures in the absence (A) and in the presence (B) of an inhibitor, IAA (10 mM). (C) Kgp on casein-coated AuNPs followed by HSA adsorption. The red dotted line indicates LOD. Mean (SD),  $n = 5$ .

for supernatants from all the four different strains of *P. gingivalis*, whereas supernatants from the non-proteolytically active *S. mutans* did not produce any shift. Hence, all samples that were shown to have significant proteolytic activity gave rise to an increase in the local RI. The LOD for the LSPR sensor was  $<0.1 \mu\text{g/mL}$  (4.3 nM), which is well below the Rgp concentrations observed in patients suffering from severe chronic periodontitis<sup>59</sup> and also below the concentrations for total protease activity in peri-implantitis<sup>49</sup> and gingivitis.<sup>61</sup> To verify the correlation between the redshift and gingipain activity, an inhibitor of Rgp and Kgp [iodoacetamide (IAA), 10 mM] was added to all samples. No clear LSPR shift was seen in any of the samples in the presence of IAA (Figure 5B), strongly indicating that gingipains were responsible for the observed LSPR redshift in the absence of IAA.

Bacteria supernatants are complex suspensions containing a wide range of proteins and other biomolecules. Although casein is widely used for blocking unspecific protein adsorption on surfaces,<sup>62</sup> casein partly degraded by proteases may not be equally efficient as a blocking agent. The LSPR redshift caused by the gingipain containing samples may thus be a result of an increase in unspecific protein accumulation as a result of casein degradation. To test this hypothesis, casein-modified AuNPs were first backfilled with HSA to ensure that no further unspecific protein binding could occur, resulting in a redshift of the LSPR band of  $1.22 \pm 0.01$  nm. The nanoparticles were then exposed to Kgp for 60 min, resulting in a concentration-

dependent blueshift as expected. Interestingly, when subjected to a second incubation in HSA (1 mg/mL), substantial redshifts were seen for all samples and that increased with the Kgp concentration (Figure 5C). The proteolytic degradation of casein hence reduced the efficiency of casein in blocking unspecific protein adsorption, providing a means to indirectly detect enzymatic activity in a complex sample matrix. Whereas the magnitude of the blueshift of the LSPR band caused by degradation of casein can never be larger than the redshift obtained when the casein was immobilized on the nanoparticles, a redshift caused by protein accumulation is only limited by the RI sensitivity and the sensing volume of the nanoparticles. The indirect detection of enzymatic activity by observing the increase in protein accumulation on the nanoparticles caused by degradation of the substrate can consequently result in larger optical shifts than what is caused by casein degradation. The redshift observed here caused by gingipain activity in the bacterial samples was about 2 nm, which was similar to what was seen also in the control experiment using recombinant Kgp followed by addition of HSA. The possibility of distinguishing samples from *P. gingivalis* that secrete active gingipains from non-proteolytically active *S. mutans* using this strategy is thus encouraging and can allow for further development of nanomaterial-based devices for simple detection of gingipains to facilitate early diagnosis of the disease onset.

## CONCLUSIONS

In this work, a nanomaterial-based multiwell format LSPR sensor for detection of gingipain activity was developed. AuNPs were immobilized in the wells and modified with casein. The casein was used as a generic protease substrate and was readily digested by both trypsin and Kgp, resulting in a concentration-dependent blueshift of the LSPR band. The LOD for the sensor was  $<0.1 \mu\text{g/mL}$  (4.3 nM), which is well below gingipain concentrations detected in severe chronic periodontitis cases. Gingipains secreted by bacteria are primarily membrane-bound, either to the outer membrane of bacteria or to vesicles. Because *P. gingivalis* resides in biofilms, only vesicle-bound gingipains will contribute to the response from samples of gingival fluid or saliva. Bacteria-free supernatants from four cultures of different strains of *P. gingivalis* were investigated and were confirmed to have high gingipain activity using fluorescence assays. In contrast to proteases in their free form, the vesicle-bound gingipains in the supernatants gave rise to a distinct redshift. No or only minor responses were seen in the presence of the gingipain inhibitor IAA or from samples from the non-proteolytically active caries bacteria *S. mutans*. Kgp digestion of a casein surface rendered them less resistant to unspecific protein adsorption. In the complex sample matrix of the bacteria supernatants, the gingipain-mediated degradation of the casein film hence resulted in accumulation of biomolecules on the sensor surface. Irrespective of this, because this accumulation only occurred in the presence of gingipain activity, it allows for indirect detection of one of the most relevant virulence factors causing periodontitis. Although the multiwell format allows for a rapid readout of multiple samples, further work will be needed to optimize and evaluate the surface chemistry and the clinical relevance. A chair-side test to analyze central biomarkers in periodontitis would be a valuable tool for enhancing periodontal diagnostics, as a complement to both radiographs and probing depth, increasing the possibility of

giving early indication of the disease onset, and estimating disease activity rather than just disease status. The possibility of monitoring gingipain activity can also indicate if treatment is successful in slowing the progression of the disease, which would add an extra dimension to the existing diagnostic tool box.

## ASSOCIATED CONTENT

### Supporting Information

The Supporting Information is available free of charge at <https://pubs.acs.org/doi/10.1021/acsnm.0c01899>.

LSPR spectra of buffers, casein degradation kinetics, and Rgp casein-FITC calibration curve (PDF)

## AUTHOR INFORMATION

### Corresponding Author

**Daniel Aili** – Laboratory of Molecular Materials, Division of Biophysics and Bioengineering, Department of Physics, Chemistry and Biology (IFM), Linköping University, 581 83 Linköping, Sweden; [orcid.org/0000-0002-7001-9415](https://orcid.org/0000-0002-7001-9415); Email: [daniel.aili@liu.se](mailto:daniel.aili@liu.se)

### Authors

**Anna Svärd** – Laboratory of Molecular Materials, Division of Biophysics and Bioengineering, Department of Physics, Chemistry and Biology (IFM), Linköping University, 581 83 Linköping, Sweden; Cardiovascular Research Centre (CVRC), School of Medical Sciences, Örebro University, 70182 Örebro, Sweden

**Jessica Neilands** – Department of Oral Biology, Faculty of Odontology, Malmö University, 205 06 Malmö, Sweden

**Eleonor Palm** – Cardiovascular Research Centre (CVRC), School of Medical Sciences, Örebro University, 70182 Örebro, Sweden

**Gunnel Svensäter** – Department of Oral Biology, Faculty of Odontology, Malmö University, 205 06 Malmö, Sweden

**Torbjörn Bengtsson** – Cardiovascular Research Centre (CVRC), School of Medical Sciences, Örebro University, 70182 Örebro, Sweden

Complete contact information is available at: <https://pubs.acs.org/doi/10.1021/acsnm.0c01899>

### Author Contributions

A.S. performed protease experiments and wrote the manuscript together with the co-authors. J.N. and G.S. contributed with FITC-casein and Zymogram data and writing for those sections. E.P. cultured and prepared bacterial supernatants and revised the manuscript. D.A. and T.B. supervised the work and revised the manuscript. The authors declare no competing financial interest.

### Notes

The authors declare no competing financial interest.

## ACKNOWLEDGMENTS

We acknowledge Professor Börje Sellergren, Malmö University, for kindly providing RgpB (GingisRex) and Kgp (GingisKHAN) gingipains via Genovis. Funding from the Swedish Research Council (VR), Dnr 2016-04874 and Dnr 2017-04475, the Swedish Foundation for Strategic Research (SFF) grant no. FFL15-0026, the Knut and Alice Wallenberg Foundation (grant no. KAW 2016.0231), is gratefully acknowledged.

## ■ REFERENCES

- (1) Kinane, D. F.; Stathopoulou, P. G.; Papapanou, P. N. Periodontal diseases. *Nat. Rev. Dis. Primers*. **2017**, *3*, 17038.
- (2) Pihlstrom, B. L.; Michalowicz, B. S.; Johnson, N. W. Periodontal diseases. *Lancet*. **2005**, *366*, 1809–1820.
- (3) Seymour, G. J.; Ford, P. J.; Cullinan, M. P.; Leishman, S.; Yamazaki, K. Relationship between periodontal infections and systemic disease. *Clin. Microbiol. Infect.* **2007**, *13*, 3–10.
- (4) Haraszthy, V. I.; Zambon, J. J.; Trevisan, M.; Zeid, M.; Genco, R. J. Identification of periodontal pathogens in atheromatous plaques. *J. Periodontol.* **2000**, *71*, 1554–1560.
- (5) Dominy, S. S.; Lynch, C.; Ermini, F.; Benedyk, M.; Marczyk, A.; Konradi, A.; Nguyen, M.; Haditsch, U.; Raha, D.; Griffin, C.; Holsinger, L. J.; Arastu-Kapur, S.; Kaba, S.; Lee, A.; Ryder, M. L.; Potempa, B.; Mydel, P.; Hellvard, A.; Adamowicz, K.; Hasturk, H.; Walker, G. D.; Reynolds, E. C.; Faull, R. L. M.; Curtis, M. A.; Dragunow, M.; Potempa, J. Porphyromonas gingivalis in Alzheimer's disease brains: Evidence for disease causation and treatment with small-molecule inhibitors. *Sci. Adv.* **2019**, *5*, No. eaau3333.
- (6) Inaba, H.; Amano, A. Roles of oral bacteria in cardiovascular diseases—from molecular mechanisms to clinical cases: Implication of periodontal diseases in development of systemic diseases. *J. Pharmacol. Sci.* **2010**, *113*, 103–109.
- (7) Genco, R. J.; Van Dyke, T. E. Reducing the risk of CVD in patients with periodontitis. *Nat. Rev. Cardiol.* **2010**, *7*, 479–480.
- (8) Kholy, K. E.; Genco, R. J.; Van Dyke, T. E. Oral infections and cardiovascular disease. *Trends Endocrinol. Metab.* **2015**, *26*, 315–321.
- (9) Chistiakov, D. A.; Orekhov, A. N.; Bobryshev, Y. V. Links between atherosclerotic and periodontal disease. *Exp. Mol. Pathol.* **2016**, *100*, 220–235.
- (10) Beck, J.; Garcia, R.; Heiss, G.; Vokonas, P. S.; Offenbacher, S. Periodontal Disease and Cardiovascular Disease. *J. Periodontol.* **1996**, *67*, 1123–1137.
- (11) Lundberg, K.; Wegner, N.; Yucel-Lindberg, T.; Venables, P. J. Periodontitis in RA—the citrullinated enolase connection. *Nat. Rev. Rheumatol.* **2010**, *6*, 727–730.
- (12) Lalla, E.; Papapanou, P. N. Diabetes mellitus and periodontitis: a tale of two common interrelated diseases. *Nat. Rev. Endocrinol.* **2011**, *7*, 738–748.
- (13) Yang, H.-W.; Huang, Y.-F.; Chou, M.-Y. Occurrence of Porphyromonas gingivalis and Tannerella forsythensis in periodontally diseased and healthy subjects. *J. Periodontol.* **2004**, *75*, 1077–1083.
- (14) Bostanci, N.; Belibasakis, G. N. Porphyromonas gingivalis: an invasive and evasive opportunistic oral pathogen. *FEMS Microbiol. Lett.* **2012**, *333*, 1–9.
- (15) How, K. Y.; Song, K. P.; Chan, K. G. Porphyromonas gingivalis: An Overview of Periodontopathic Pathogen below the Gum Line. *Front. Microbiol.* **2016**, *7*, 53.
- (16) Fitzpatrick, R. E.; Wijeyewickrema, L. C.; Pike, R. N. The gingipains: scissors and glue of the periodontal pathogen, Porphyromonas gingivalis. *Future Microbiol.* **2009**, *4*, 471–487.
- (17) Guo, Y.; Nguyen, K. A.; Potempa, J. Dichotomy of gingipains action as virulence factors: from cleaving substrates with the precision of a surgeon's knife to a meat chopper-like brutal degradation of proteins. *Periodontology* **2010**, *54*, 15–44.
- (18) Hajishengallis, G. Complement and periodontitis. *Biochem. Pharmacol.* **2010**, *80*, 1992–2001.
- (19) Popadiak, K.; Potempa, J.; Riesbeck, K.; Blom, A. M. Biphasic effect of gingipains from Porphyromonas gingivalis on the human complement system. *J. Immunol.* **2007**, *178*, 7242–7250.
- (20) Potempa, J.; Pike, R.; Travis, J. Titration and mapping of the active site of cysteine proteinases from Porphyromonas gingivalis (gingipains) using peptidyl chloromethanes. *Biol. Chem.* **1997**, *378*, 223–230.
- (21) Potempa, J.; Pike, R.; Travis, J. The multiple forms of trypsin-like activity present in various strains of Porphyromonas gingivalis are due to the presence of either Arg-gingipain or Lys-gingipain. *Infect. Immun.* **1995**, *63*, 1176–1182.
- (22) Xiang, X.; Sowa, M. G.; Iacopino, A. M.; Maev, R. G.; Hewko, M. D.; Man, A.; Liu, K.-Z. An update on novel non-invasive approaches for periodontal diagnosis. *J. Periodontol.* **2010**, *81*, 186–198.
- (23) van Winkelhoff, A. J.; van der Velden, U.; Clement, M.; de Graaff, J. Intra-oral distribution of black-pigmented Bacteroides species in periodontitis patients. *Oral Microbiol. Immunol.* **1988**, *3*, 83–85.
- (24) Slots, J.; Hafstrom, C.; Rosling, B.; Dahlen, G. Detection of Actinobacillus actinomycetemcomitans and Bacteroides gingivalis in subgingival smears by the indirect fluorescent-antibody technique. *J. Periodontol. Res.* **1985**, *20*, 613–620.
- (25) Boutaga, K.; van Winkelhoff, A. J.; Vandembroucke-Grauls, C. M. J. E.; Savelkoul, P. H. M. Comparison of real-time PCR and culture for detection of Porphyromonas gingivalis in subgingival plaque samples. *J. Clin. Microbiol.* **2003**, *41*, 4950–4954.
- (26) Sakamoto, M.; Takeuchi, Y.; Umeda, M.; Ishikawa, I.; Benno, Y. Rapid detection and quantification of five periodontopathic bacteria by real-time PCR. *Microbiol. Immunol.* **2001**, *45*, 39–44.
- (27) Galassi, F.; Kaman, W. E.; Anssari Moin, D.; van der Horst, J.; Wismeijer, D.; Crielaard, W.; Laine, M. L.; Veerman, E. C. I.; Bikker, F. J.; Loos, B. G. Comparing culture, real-time PCR and fluorescence resonance energy transfer technology for detection of Porphyromonas gingivalis in patients with or without peri-implant infections. *J. Periodontol. Res.* **2012**, *47*, 616–625.
- (28) Alhogail, S.; Suaifan, G. A. R. Y.; Bizzarro, S.; Kaman, W. E.; Bikker, F. J.; Weber, K.; Cialla-May, D.; Popp, J.; Zourob, M. On site visual detection of Porphyromonas gingivalis related periodontitis by using a magnetic-nanobead based assay for gingipains protease biomarkers. *Mikrochim. Acta* **2018**, *185*, 149.
- (29) Mäntylä, P.; Stenman, M.; Kinane, D. F.; Tikanoja, S.; Luoto, H.; Salo, T.; Sorsa, T. Gingival crevicular fluid collagenase-2 (MMP-8) test stick for chair-side monitoring of periodontitis. *J. Periodontol. Res.* **2003**, *38*, 436–439.
- (30) McCulloch, C. A. G. Host enzymes in gingival crevicular fluid as diagnostic indicators of periodontitis. *J. Clin. Periodontol.* **1994**, *21*, 497–506.
- (31) Cullinan, M.; Ford, P.; Seymour, G. Periodontal disease and systemic health: current status. *Aust. Dent. J.* **2009**, *54*, S62–S69.
- (32) Seymour, R. A. Is gum disease killing your patient? *Br. Dent. J.* **2009**, *206*, 551–552.
- (33) Saha, K.; Agasti, S. S.; Kim, C.; Li, X.; Rotello, V. M. Gold nanoparticles in chemical and biological sensing. *Chem. Rev.* **2012**, *112*, 2739–2779.
- (34) Li, Y.; Schluesener, H. J.; Xu, S. Gold nanoparticle-based biosensors. *Gold Bull.* **2010**, *43*, 29–41.
- (35) Hutter, E.; Maysinger, D. Gold-nanoparticle-based biosensors for detection of enzyme activity. *Trends Pharmacol. Sci.* **2013**, *34*, 497–507.
- (36) Oliveira-Silva, R.; Sousa-Jerónimo, M.; Botequim, D.; Silva, N. J. O.; Paulo, P. M. R.; Prazeres, D. M. F. Monitoring Proteolytic Activity in Real Time: A New World of Opportunities for Biosensors. *Trends Biochem. Sci.* **2020**, *45*, 604–618.
- (37) Zhen, Z.; Tang, L.-J.; Long, H.; Jiang, J.-H. Enzymatic immuno-assembly of gold nanoparticles for visualized activity screening of histone-modifying enzymes. *Anal. Chem.* **2012**, *84*, 3614–3620.
- (38) Sun, C.; Su, K.-H.; Valentine, J.; Rosa-Bauza, Y. T.; Ellman, J. A.; Elboudwarej, O.; Mukherjee, B.; Craik, C. S.; Shuman, M. A.; Chen, F. F.; Zhang, X. Time-resolved single-step protease activity quantification using nanoplasmonic resonator sensors. *ACS Nano* **2010**, *4*, 978–984.
- (39) Lorén, A.; Engelbrektsson, J.; Eliasson, C.; Josefson, M.; Abrahamsson, J.; Johansson, M.; Abrahamsson, K. Internal standard in surface-enhanced Raman spectroscopy. *Anal. Chem.* **2004**, *76*, 7391–7395.
- (40) Halas, N. J.; Haes, A. J.; Van Duyne, R. P. Nanoscale optical biosensors based on localized surface plasmon resonance spectroscopy. *Proc. SPIE* **2003**, *5221*, 47.

- (41) Hong, Y.; Ku, M.; Lee, E.; Suh, J.-S.; Huh, Y.-M.; Yoon, D. S.; Yang, J. Localized surface plasmon resonance based nanobiosensor for biomarker detection of invasive cancer cells. *J. Biomed. Optic.* **2014**, *19*, 051202.
- (42) Chen, H.; Kou, X.; Yang, Z.; Ni, W.; Wang, J. Shape- and size-dependent refractive index sensitivity of gold nanoparticles. *Langmuir* **2008**, *24*, 5233–5237.
- (43) Unser, S.; Bruzas, I.; He, J.; Sagle, L. Localized Surface Plasmon Resonance Biosensing: Current Challenges and Approaches. *Sensors*. **2015**, *15*, 15684–15716.
- (44) Hutter, E.; Fendler, J. H. Exploitation of Localized Surface Plasmon Resonance. *Adv. Mater.* **2004**, *16*, 1685–1706.
- (45) Nooney, R. I.; Stranik, O.; McDonagh, C.; MacCraith, B. D. Optimization of plasmonic enhancement of fluorescence on plastic substrates. *Langmuir* **2008**, *24*, 11261–11267.
- (46) Decher, G. Fuzzy nanoassemblies: Toward layered polymeric multicomposites. *Science* **1997**, *277*, 1232–1237.
- (47) Mayer, K. M.; Hafner, J. H. Localized surface plasmon resonance sensors. *Chem. Rev.* **2011**, *111*, 3828–3857.
- (48) Martinsson, E.; Otte, M. A.; Shahjamali, M. M.; Sepulveda, B.; Aili, D. Substrate Effect on the Refractive Index Sensitivity of Silver Nanoparticles. *J. Phys. Chem. C* **2014**, *118*, 24680–24687.
- (49) Neilands, J.; Wickström, C.; Kinnby, B.; Davies, J. R.; Hall, J.; Friberg, B.; Svensäter, G. Bacterial profiles and proteolytic activity in peri-implantitis versus healthy sites. *Anaerobe* **2015**, *35*, 28–34.
- (50) Chen, P.; Liu, X.; Goyal, G.; Tran, N. T.; Shing Ho, J. C.; Wang, Y.; Aili, D.; Liedberg, B. Nanoplasmonic Sensing from the Human Vision Perspective. *Anal. Chem.* **2018**, *90*, 4916–4924.
- (51) French, M. Serum IgG subclasses in normal adults. *Monogr. Allergy* **1986**, *19*, 100–107.
- (52) Vincents, B.; Guentsch, A.; Kostolowska, D.; Pawel-Rammingen, U.; Eick, S.; Potempa, J.; Abrahamson, M. Cleavage of IgG1 and IgG3 by gingipain K from *Porphyromonas gingivalis* may compromise host defense in progressive periodontitis. *FASEB J.* **2011**, *25*, 3741–3750.
- (53) Sundqvist, G.; Carlsson, J.; Herrmann, B.; Tarnvik, A. Degradation of human immunoglobulins G and M and complement factors C3 and C5 by black-pigmented *Bacteroides*. *J. Med. Microbiol.* **1985**, *19*, 85–94.
- (54) Sroka, A.; Sztukowska, M.; Potempa, J.; Travis, J.; Genco, C. A. Degradation of host heme proteins by lysine- and arginine-specific cysteine proteinases (gingipains) of *Porphyromonas gingivalis*. *J. Bacteriol.* **2001**, *183*, 5609–5616.
- (55) Potempa, J.; Mikolajczyk-Pawlinska, J.; Brassell, D.; Nelson, D.; Thøgersen, I. B.; Enghild, J. J.; Travis, J. Comparative properties of two cysteine proteinases (gingipains R), the products of two related but individual genes of *Porphyromonas gingivalis*. *J. Biol. Chem.* **1998**, *273*, 21648–21657.
- (56) Pathirana, RD; O'Brien-Simpson, NM; Reynolds, EC Host immune responses to *Porphyromonas gingivalis* antigens. *Periodontology* **2010**, *52*, 218–237.
- (57) Lamont, R. J.; Jenkinson, H. F. Life below the gum line: pathogenic mechanisms of *Porphyromonas gingivalis*. *Microbiol. Mol. Biol. Rev.* **1998**, *62*, 1244–1263.
- (58) Bengtsson, T.; Khalaf, A.; Khalaf, H. Secreted gingipains from *Porphyromonas gingivalis* colonies exert potent immunomodulatory effects on human gingival fibroblasts. *Microbiol. Res.* **2015**, *178*, 18–26.
- (59) Guentsch, A.; Kramesberger, M.; Sroka, A.; Pfister, W.; Potempa, J.; Eick, S. Comparison of gingival crevicular fluid sampling methods in patients with severe chronic periodontitis. *J. Periodontol.* **2011**, *82*, 1051–1060.
- (60) Lönn, J.; Johansson, C. S.; Nakka, S.; Palm, E.; Bengtsson, T.; Nayeri, F.; Ravald, N. High concentration but low activity of hepatocyte growth factor in periodontitis. *J. Periodontol.* **2014**, *85*, 113–122.
- (61) Figueredo, C. M. S.; Gustafsson, A. Protease activity in gingival crevicular fluid: presence of free protease. *J. Clin. Periodontol.* **1998**, *25*, 306–310.
- (62) Tacha, D. E.; McKinney, L. Casein reduces nonspecific background staining in immunolabeling techniques. *J. Histotechnol.* **1992**, *15*, 127–132.